Quasifree knockout in $^{16}O(p,2p)^{15}N$ at an incident energy of 151 MeV

A. A. Cowley, J. J. Lawrie, G. C. Hillhouse, D. M. Whittal, S. V. Förtsch, J. V. Pilcher, and F. D. Smit
National Accelerator Centre, Faure, 7131, South Africa

P. G. Roos
Department of Physics and Astronomy, University of Maryland, College Park, Maryland 20742
(Received 18 January 1991)

Cross sections for the reaction $^{16}O(p,2p)^{15}N$ to the ground state and excited state at 6.32 MeV have been measured at an incident energy of 151 MeV. The data are in good agreement with distorted-wave impulse-approximation calculations. The factorization approximation is found to be valid for the region of phase space studied. The extracted spectroscopic factors are reasonably consistent with those determined in other experiments, and they are also compatible with results of a weak-coupling nuclear structure model.

I. INTRODUCTION

Knockout reactions have in the past proved to be invaluable with regard to their ability to provide information on nucleon-hole states in nuclei. In recent years interest has been focused on the theoretical description of the reaction at incident proton energies where distortion effects are severe, and where various aspects of the commonly used distorted-wave impulse-approximation (DWIA) calculations consequently need to be treated with caution. However, in spite of doubts about the factorization approximation for $^{16}O(p,2p)$ at an incident energy of 200 MeV [1], Samanta *et al.* [2] find evidence for its validity at energies even as low as 80 MeV for $^{40}Ca(p,2p)$. This is understood to be a result of attenuation and phasing effects of the distortion, which together ensure strong surface localization. Consequently, the requirements for the validity of the factorization approximation are satisfied because of the limited surface region which contributes the major yield to the differential cross section.

Samanta *et al.* [2] report spectroscopic factors for $^{16}O(p,2p)^{15}N$ at an incident energy of 100 MeV for the ground state ($\frac{1}{2}^-$) and excited state ($\frac{3}{2}^-$, 6.32 MeV) which are in reasonable agreement with results of pick-up reactions, and with expectations for the closed-shell limit. On the other hand, the spectroscopic factors obtained in their work are in disagreement with values [1] found for $^{16}O(p,2p)$ at an incident energy of 200 MeV. Obviously, the unavailability of reliable energy-dependent optical potentials for a consistent treatment of the distortion in a system as light as ^{16}O, is a likely cause [1] of the scatter in the extracted spectroscopic factors. In addition, Samanta *et al.* [2] explain how the values of the extracted spectroscopic factors at 200 MeV could have been affected by the poor energy resolution in the experiment of Kitching *et al.* [1].

The present study was initiated to investigate the reaction $^{16}O(p,2p)$ at an incident energy of 150 MeV, in order to have additional data at an energy intermediate to the existing results at 100 and 200 MeV. This experiment, together with the previous work, allows us to explore the incident-energy dependence over a range where distortion effects change drastically, in the same way as was previously studied for ^{40}Ca in Ref. [2].

II. EXPERIMENTAL PROCEDURE

A proton beam of 151 ± 0.5 MeV was delivered by the separated-sector cyclotron [3] of the National Accelerator Centre to a 1.5-m-diameter scattering chamber in which the target and detectors were mounted. The oxygen gas ($>99.9\%$ purity, 99.8% ^{16}O) was contained in a cylindrical gas cell of diameter 10 cm and height 4 cm, with entrance and exit windows of 6-μm Havar foil. The pressure in the gas cell was maintained at slightly above atmospheric pressure and was monitored to a precision of better than 1%. The gas in the cell was assumed to remain in thermal equilibrium with its environment.

The three detector telescopes were arranged in an in-plane configuration with one telescope on a movable arm on one side of the beam, and the other two telescopes (separated by 15°) mounted on a second movable arm which covered an angular range of 50° to 70° on the other side. Double-aperture brass collimators in front of each detector telescope (1-mm Si surface-barrier detector, followed by 51-mm diameter by 127-mm-long NaI crystal-phototube assembly with a thin entrance window) defined the effective target lengths and solid angles. The coincidence target length between the one primary telescope and the two secondary telescopes varied between 8 and 10 mm. The effective angular resolution was 4°. The collimators subtended 3.8 msr at the center of the target, with distances of 135 mm between the front vertical slits and the circular rear apertures of diameter 14 mm. The front slits had widths of 18 mm (primary) and 5 mm (secondary telescopes).

Standard fast-coincidence electronics were used to process the signals from the detectors and these pulses were then processed by an on-line computer which also wrote event-by-event tape for subsequent off-line analysis. Light-emitting diodes (LED) implanted in the NaI crystals were triggered at a rate proportional to the beam current and the light output from these was used to stabilize the gains of the photomultiplier tubes. Tail pulses were also introduced to the preamplifiers of the Si detectors and these were used, together with the LED pulses from the NaI detectors, for correction of electronic dead time and pileup.

Energy calibrations of the Si detectors were based on α particles from a ^{228}Th source, and the slightly nonlinear calibrations of the NaI detectors were determined from protons scattered elastically from a thin plastic target. The angular offsets of the detector telescopes from their nominal values were measured by means of forward-angle elastic scattering on either side of the beam, combined with the observed angular separation of the p-^{2}H coincidence yield from the reaction ^{2}H$(p,p)^2$H in a deuterated plastic target. Particle identification was based on the standard ΔE-E technique.

Correction for accidental coincidences in the prompt timing peak was performed by subtracting events from neighboring beam bursts of the cyclotron rf structure. To correct for reaction losses in the NaI crystals, we used the empirical formula of Green, Boal, Helmer, Jackson, and Korteling [4], which gives values for the reaction tail within 2% of Cameron *et al.* [5] at 89 and 104 MeV, and a value within 3% of that quoted in the Janni tables [6] for 150 MeV protons in NaI. Sources and magnitudes of systematic errors are similar to those listed in Ref. 7. Thus the uncertainty of the absolute cross section scales is less than 10%.

Data were taken at the angle pairs listed in Table I. A typical binding energy spectrum, with a missing-mass resolution of 2 MeV, is shown in Fig. 1. This spectrum was derived from

$$E_{\text{total}} = T_1 + T_2 + T_3 ,$$

where T_1 and T_2 are the kinetic energies of the observed protons, and T_3 is the calculated energy of the unobserved recoiling nucleus. Compared with results at 100

TABLE I. Angle pairs (θ_1,θ_2) and (θ_1,θ_3) at which energy-sharing distributions were measured. Different signs indicate opposite sides of the beam. The minimum recoil momentum $P_{\min}$ which is kinematically allowed is indicated for each angle pair.

θ_1 (deg)	$-\theta_2$ (deg)	$P_{\min}$ (MeV/c)	$-\theta_3$ (deg)	$P_{\min}$ (MeV/c)
34.6	54.2	28	69.4	91
38.7	46.9	14	62.1	81
40.6	50.7	39	65.9	108
43.1	54.2	67	69.4	138
47.3	46.9	53	62.1	127
47.3	54.2	88	69.4	163

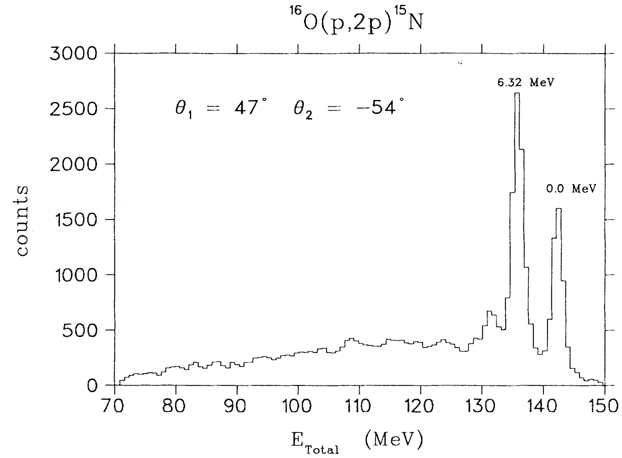

FIG. 1. Binding-energy spectrum for the reaction ^{16}O$(p,2p)^{15}$N at an incident energy of 151 MeV.

MeV [2], the unresolved $\frac{5}{2}^+$(5.27 MeV) and $\frac{1}{2}^+$(5.299 MeV) doublet may have an even lower yield relative to the other states in ^{15}N. This behavior would be consistent with the trend observed [8] for similar final states in ^{11}B. These states cannot be reached by means of a one-step process, therefore their excitation is expected to decrease with increasing incident energy.

III. DWIA ANALYSIS

In a factorized DWIA, the cross section for a reaction $A(a,a'b)B$ is given [9] by

$$\frac{d^3\sigma}{d\Omega_{a'}\,d\Omega_b\,dE_{a'}} = S_b F_k \frac{d\sigma}{d\Omega_{a-b}} \sum_{\Lambda} |T_L^{\Lambda}|^2 , \qquad (1)$$

where S_b is the spectroscopic factor for the bound proton b, F_k is a kinematic factor, and $(d\sigma/d\Omega)_{a-b}$ is a half-shell two-body cross section for a-b scattering. The quantity $\sum_\Lambda |T_L^\Lambda|^2$ is a distorted momentum distribution for b in target A, where

$$T_L^{\Lambda} = (2L+1)^{-1/2} \times \int \chi_{a'}^{(-)*}(\mathbf{r})\chi_b^{(-)*}(\mathbf{r})\Phi_L^{\Lambda}(\mathbf{r})\chi_a^{(+)}\left[\frac{B}{A}\mathbf{r}\right] d\mathbf{r} . \qquad (2)$$

In Eq. (2) the χ's are distorted waves for the incident and emitted particles and $\Phi_L^\Lambda(\mathbf{r})$ is the relative-motion wave function for b and B in the target A. For the relative angular momentum $L \neq 0$ the struck proton, in general, has an effective polarization due to the central parts of the complex optical potentials, which is normal to the scattering plane [10]. This result holds even with spin-orbit distortion neglected. Hence, the two-body cross section used in Eq. (1) is then replaced by

$$\frac{d\sigma}{d\Omega}=\frac{d\sigma}{d\Omega}\bigg|_{\text{unpol}}(1+PA)\,, \qquad (3)$$

where A is the two-body analyzing power and the effective polarization P is calculable in DWIA.

In our analysis spin-orbit terms are included in the optical potentials. Therefore the resultant distorted waves become matrices in spin space $\chi^{\pm}_{\rho\sigma}$ and Eq. (1) has the form [11]

$$\frac{d^3\sigma}{d\Omega_{a'}\,d\Omega_b\,dE_{a'}}=S_bF_{k'}\sum_{\substack{M\\ \rho_a\rho_{a'}\rho_{b'}}}\left|\sum_{\substack{\Lambda\rho_b\\ \sigma_a\sigma_{a'}\sigma_{b'}}}(L\Lambda\tfrac{1}{2}\rho_b|JM)(2L+1)^{1/2}T^{L\Lambda}_{\substack{\rho_a\rho_{a'}\rho_{b'}\\ \sigma_a\sigma_{a'}\sigma_{b'}}}\langle\sigma_{a'}\sigma_{b'}|t|\sigma_a\rho_b\rangle\right|^2 . \qquad (4)$$

Here $F_{k'}$ is a kinematic factor, ρ_i and σ_i are spin projections for particle i, and b' refers to particle b in the exit channel. In this case the a-b t matrix, although still factored out of the distorted-wave integral, cannot be removed from the coherent sum. Consequently, the calculation of the cross section becomes more complicated.

In the calculations, which were performed with the code THREEDEE [12], nonlocality of the optical potentials was treated in a conventional manner by introducing a damping factor $\exp[\beta^2\mu V(r)/4\hbar^2]$ for each distorted wave, where $V(r)$ is the equivalent local potential, β is the range of nonlocality, and μ the reduced mass. Values of the two-body t matrix for p-p scattering were obtained from an interpolation of available nucleon-nucleon phase shifts and the p-p scattering was evaluated at the final proton-proton rest energy (final energy prescription). At the incident energy and angles examined in the present study, results with the initial and final energy prescriptions differ by less than 5%.

Distorted waves were generated with the global optical potentials of Nadasen *et al.* [13] and the bound state was calculated with the potential parameters of Elton and Swift [14]. Although the parameters of Nadasen *et al.* were derived for medium to heavy target masses, these were chosen in our analysis because of the rather good fits provided to earlier data on $^{16}O(p,2p)^{15}N$ at 100 MeV [2]. The similar potentials of Schwandt *et al.* [15], which are based on a more extensive set of experimental data, and which to some extent supersede those of Ref. [13], are also available. However, the need for a consistent comparison with the previous study [2] of $^{16}O(p,2p)^{15}N$ at 100 MeV influenced our choice of potentials. For a similar reason the potentials of Abdul-Jalil and Jackson [16], which are appropriate for light target masses, were not used. Nevertheless, as a check on the possible effect of a different set of optical potentials, a calculation with the parameters of Ref. 16 was performed for the angle pair at which the lowest minimum recoil momentum occurs ($\theta_1=39°$, $\theta_2=-47°$). This resulted in poor shape agreement with our experimental data, which casts doubt on the value of the ($\sim$40% lower) extracted spectroscopic factor.

IV. RESULTS AND DISCUSSION

Energy-sharing distributions, i.e., differential cross sections for the individual residual states plotted as a function of the kinetic energy of one of the detected protons, are shown in Figs. 2 and 3. Results are grouped according to the value of the angle of one of the detected protons. We find that the energy-sharing distributions usually show a dip, which is most pronounced at angle pairs where low recoil momentum is kinematically allowed. As the second angle assumes a value different from the quasifree angle, the dip gradually washes out until it disappears entirely. For a primary angle of 69°, for example, the data represent only the region beyond the maxima, as recoil momenta lower than a certain value are not attainable.

The experimental energy-sharing distributions, which are consistent with $L\neq0$ transitions, are reproduced well by the DWIA calculations. Only calculations with spin-orbit terms in the optical potentials, and with nonlocality corrections for incident and scattered waves are shown.

Normalization factors, which represent the extracted spectroscopic factors, are determined for each energy-sharing distribution, and are given in Figs. 2 and 3. Clearly, a single value of this factor would be appropriate, and consequently the observed spread in values must be a result of the inherent inaccuracy in the procedure, as well as intrinsic inadequacies in the theory. However, it is found that the maximum deviation from the simple arithmetic mean is reasonably small ($\pm$15%) for the reaction to the ground state. This is also true for the 6.32-MeV excited state of ^{15}N if the extreme value for θ_1, $\theta_2=47°$, $-69°$ is excluded.

Average spectroscopic factors obtained in this work are listed in Table II, where results from other studies are also included. In addition to this, new spectroscopic values for $^{16}O(p,2p)^{15}N$ at an incident energy of 100 MeV are obtained from a reanalysis of the data of Samanta *et al.* [2] in order to remove minor discrepancies between our specific calculational treatment and the earlier analysis. This causes a $\sim 15\%$ downward adjustment of the earlier spectroscopic factors, but this decrease should only be regarded as giving an indication of the uncertainty associated with the extraction of values for the spectroscopic factors. It should also be noted that a reanalysis [17] of the $^{16}O(p,2p)^{15}N$ results at 200 MeV

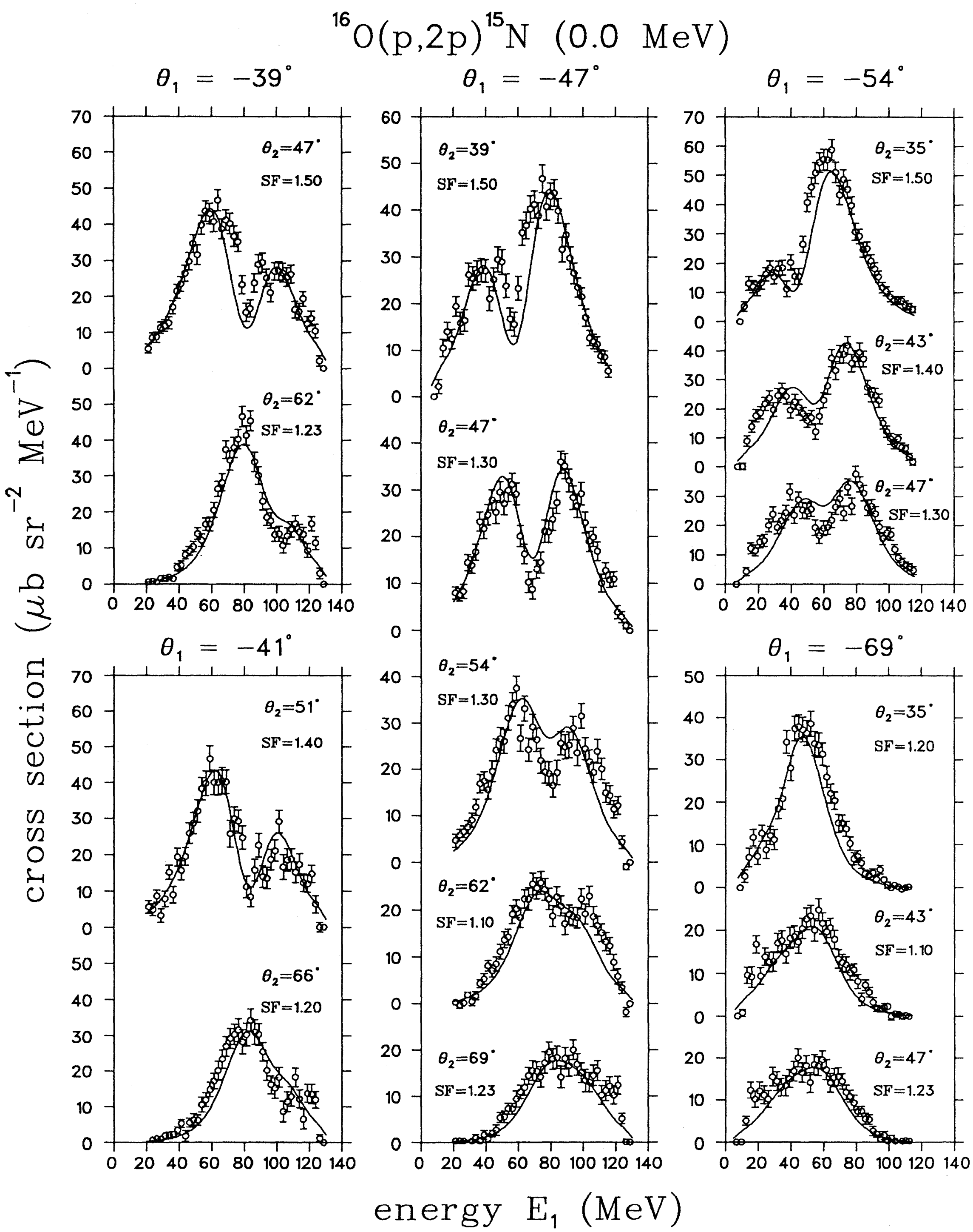

FIG. 2. Energy-sharing distributions for $^{16}O(p,2p)^{15}N$ (0.0 MeV) at an incident energy of 151 MeV measured at angle pairs (θ_1,θ_2). The curves are results of distorted-wave impulse-approximation (DWIA) calculations with the indicated spectroscopic factors (SF). Results are given in the laboratory coordinate system and statistical error bars are shown.

gives essentially the same results as the original values of Kitching *et al.* [1], although the agreement with the experimental analyzing powers is superior. In this case only the results of the improved analysis of Kudo and Miyazaki [17] are included in Table II.

Although there appears to be a slight decrease in the value of the spectroscopic factor with incident energy for the reaction $^{16}O(p,2p)^{15}N$ (g.s.), this variation is probably

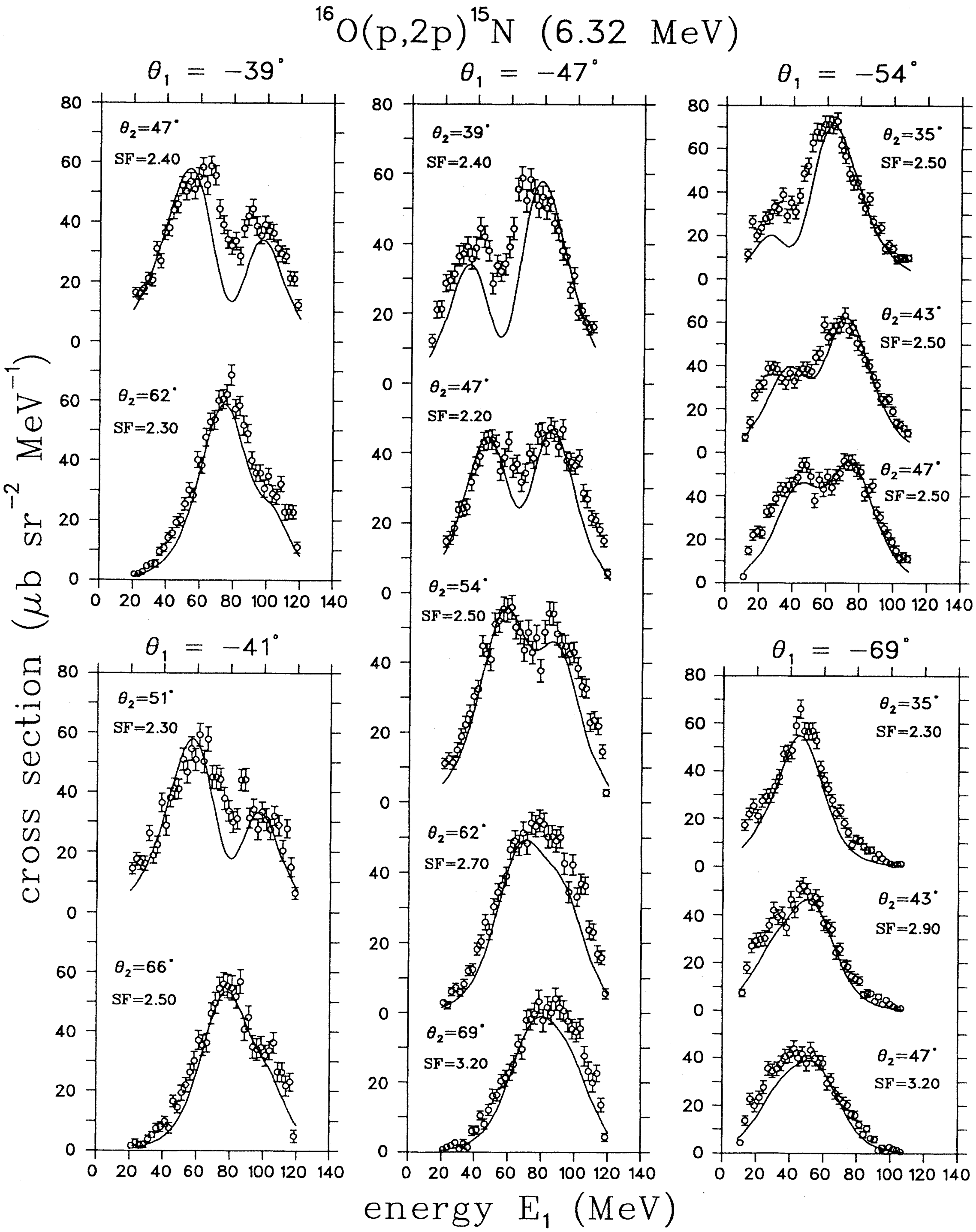

FIG. 3. Energy-sharing distributions for $^{16}O(p,2p)^{15}N$ (6.32 MeV). See caption to Fig. 2.

TABLE II. Average spectroscopic factors.

Reaction	Incident energy (MeV)	Reference	Spectroscopic factors $^{15}N_{g.s.}(\frac{1}{2}^-)$	$^{15}N_{6.3}(\frac{3}{2}^-)$
$(p,2p)$	101	2	2.2	3.1
	101	2[a]	1.9	2.5
	151	This work	1.3	2.4
	200	17	1.3	2.7
$(e,e'p)$	500	18[b]	1.2	2.3
$(d,^3He)$	29	20	2.2–2.3	2.8–3.7
	34	21	2.1	3.7
Theory		19	1.5	2.9

[a]Our reanalysis of the results of Ref. 2. [b]Values from Ref. [18] corresponding to Elton-Swift [14] bound state, and with spin-orbit interaction in distorting potentials.

not significant if the uncertainties in the values are considered. For the reaction $^{16}O(p,2p)^{15}N^*$ the variation is negligible ($\leq 7\%$). Furthermore, the values obtained for the spectroscopic factor for the $(p,2p)$ reaction are in agreement with those of an $(e,e'p)$ study [18], as well as with those of the weak-coupling nuclear structure model [19]. The values for $(d,^3He)$ are generally higher [20,21].

Calculations with the factorized DWIA [Eq. (1)] gave spectroscopic values which were similar to those indicated in Figs. 2 and 3. The small spread in the values implies that the factorization approximation is rather good. This result is more clearly demonstrated in Fig. 4, where the following quantity is shown:

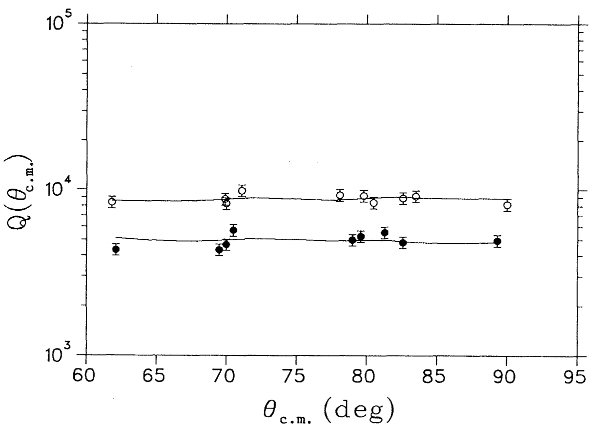

FIG. 4. The quantity Q extracted at the peaks of the energy-sharing distributions for $^{16}O(p,2p)^{15}N$ at 151 MeV to the ground state (solid circles) and excited state at 6.32 MeV (open circles) as a function of the two-body center-of-mass scattering angle. The curves are given by Eq. (6), with spectroscopic factors from Table II.

$$Q(\theta_1,\theta_2)=\frac{d^3\sigma(\theta_1,\theta_2)}{d\Omega_{a'}\,d\Omega_b\,dE_{a'}}\left[F_k\sum_{\Lambda}\left|T_L^{\Lambda}\right|^2\right]^{-1}, \quad (5)$$

where

$$\frac{d^3\sigma(\theta_1,\theta_2)}{d\Omega_{a'}\,d\Omega_b\,dE_{a'}}$$

is the experimental three-body cross section. The quantity Q, which is constructed under the assumption that spin-orbit distortions may be neglected, is given by

$$Q(\theta_1,\theta_2)=S_b\frac{d\sigma}{d\Omega_{a\text{-}b}}(1+AP) \quad (6)$$

if the factorization approximation is satisfactory, and this quantity for p-p scattering is also plotted in Fig. 4. Clearly, the factorization approximation is satisfied to a high degree in this reaction.

V. CONCLUSION

As expected, the DWIA was found to give a reasonable account of experimental energy-sharing distributions for the reaction $^{16}O(p,2p)^{15}N$ to the ground state and excited state at 6.32 MeV. Spectroscopic factors are reasonably independent of incident energy, and are also consistent with results from electron knockout studies. These values are considerably smaller than those expected for a simple closed-shell model, but are in agreement with the weak-coupling nuclear structure model.

It is concluded that previous concerns regarding the apparent discrepancy in the results for $^{16}O(p,2p)$ at 100 and 200 MeV are probably not justified. Although there might be a need for better optical potentials in the analysis, the available set of parameters do not seem to be inappropriate.

ACKNOWLEDGMENTS

We thank C. J. Stevens and V. C. Wikner for technical assistance. One of us (P.G.R.) acknowledges the hospitality extended by the National Accelerator Centre.

[1] P. Kitching, C. A. Miller, D. A. Hutcheon, A. N. James, W. J. McDonald, J. M. Cameron, W. C. Olsen, and G. Roy, Phys. Rev. Lett. **37**, 1600 (1976); P. Kitching, C. A. Miller, W. C. Olsen, D. A. Hutcheon, W. J. McDonald, and A. W. Stetz, Nucl. Phys. **A340**, 423 (1980).

[2] C. Samanta, N. S. Chant, P. G. Roos, A. Nadasen, J. Wesick, and A. A. Cowley, Phys. Rev. C **34**, 1610 (1986).

[3] A. H. Botha, H. N. Jungwirth, J. J. Kritzinger, D. Reitmann, and S. Schneider in *Proceedings of the Eleventh International Conference on Cyclotrons and their Applications, Tokyo, 1986,* edited by M. Sekiguchi, Y. Yano, and K. Hatanaka (Ionics Publishing Co., Tokyo, 1987), p. 9; J. V. Pilcher, A. A. Cowley, D. M. Whittal, and J. J. Lawrie, Phys. Rev. C **40**, 1937 (1989).

[4] R. E. L. Green, D. H. Boal, R. L. Helmer, K. P. Jackson, and R. G. Korteling, Nucl. Phys. **A405**, 463 (1983).

[5] J. M. Cameron, P. Kitching, R. H. McCamis, C. A. Miller, G. A. Moss, J. G. Rogers, G. Roy, A. W. Stetz, C. A. Goulding, and W. T. H. van Oers, Nucl. Instrum. Methods **143**, 399 (1977).

[6] Joseph F. Janni, At. Data Nucl. Data Tables **27**, 147 (1982).

[7] D. M. Whittal, A. A. Cowley, J. V. Pilcher, S. V. Förtsch, F. D. Smit, and J. J. Lawrie, Phys. Rev. C **42**, 309 (1990).

[8] H. G. Pugh, D. L. Hendrie, Marc Chabre, and E. Boschitz, Phys. Rev. **155**, 1054 (1967); D. W. Devins, D. L. Friesel, W. P. Jones, A. C. Attard, I. D. Svalbe, V. C. Officer, R. S. Henderson, B. M. Spicer, and G. G. Shute, Aust. J. Phys. **32**, 323 (1979).

[9] N. S. Chant and P. G. Roos, Phys. Rev. C **15**, 57 (1977).

[10] G. Jacob, Th. A. J. Maris, C. Schneider, and M. R. Teodoro, Phys. Lett. **45B**, 181 (1973); Nucl. Phys. **A257**, 517 (1976).

[11] N. S. Chant, P. Kitching, P. G. Roos, and L. Antonuk, Phys. Rev. Lett. **43**, 495 (1979); N. S. Chant and P. G. Roos, Phys. Rev. C **27**, 1060 (1983); N. S. Chant, in *The Interaction Between Medium Energy Nucleons in Nuclei—1982, IUCF,* edited by H. O. Meyer, AIP Conf. Proc. No. 97 (AIP, New York, 1983), p. 205.

[12] N. S. Chant, code THREEDEE, University of Maryland (unpublished).

[13] A. Nadasen, P. Schwandt, P. P. Singh, W. W. Jacobs, A. D. Bacher, P. T. Debevec, M. D. Kaitchuck, and J. T. Meek, Phys. Rev. C **23**, 1023 (1981).

[14] L. R. B. Elton and A. Swift, Nucl. Phys. **A94**, 52 (1967).

[15] P. Schwandt, H. O. Meyer, W. W. Jacobs, A. D. Bacher, S. E. Vigdor, M.D. Kaitchuck, and T. R. Donoghue, Phys. Rev. C **26**, 55 (1982).

[16] I. Abdul-Jalil and Daphne F. Jackson, J. Phys. G **5**, 1699 (1979).

[17] Yoshiteru Kudo and Kiro Miyazaki, Phys. Rev. C **34**, 1192 (1986).

[18] M. Bernheim *et al.*, Nucl. Phys. **A375**, 381 (1982).

[19] M. A. Firestone, J. Jänecke, A. Dudek-Ellis, P. J. Ellis, and T. Engeland, Nucl. Phys. **A258**, 317 (1976).

[20] J. D. Cossairt, S. B. Talley, D. P. May, R. E. Tribble, and R. L. Spross, Phys. Rev. C **18**, 23 (1978).

[21] J. C. Hiebert, E. Newman, and R. H. Bassel, Phys. Rev. **154**, 898 (1967).